FUDMA Journal of Sciences (FJS)
ISSN online: 2616-1370
ISSN print: 2645 - 2944
Vol. 10 No. 2, January, 2026, pp 326 – 331
DOI: https://doi.org/10.33003/fjs-2026-1002-4667

ANALYTICAL SOLUTIONS FOR STRESSES AND DISPLACEMENTS IN ROTATING SOLID AND HOLLOW SPHERES UNDER INTERNAL PRESSURE

***[1]Ekeadinotu, Chibueze Barnabas, [2]Erumaka, Ephraim Ngozi, [3]Chukwuchekwa, Joy Ulumma, [4]Nwagwu, Isaac Ogazie and [5]Amalahu, Christian Chinenye**

[1]Department of Mathematics, University of Agriculture and Environmental Sciences, Umuagwo Imo State, Nigeria.
[2]Department of Mathematics, Federal University of Technology, Owerri, Imo State, Nigeria.
[3]Department of Mathematics, Federal University of Technology, Owerri, Imo, Nigeria.
[4]Department of Mathematics, Federal University of Technology, Owerri, Imo State, Nigeria.
[5]Department of Mathematics, University of Agriculture and Environmental Sciences, Umuagwo Imo State, Nigeria.

*Corresponding authors' email: chibuezeekeadinotu@gmail.com

ABSTRACT

This study determines the exact solution through which stresses and displacements in both solid and hollow sphere rotates under internal pressure. We use an indirect method, which assumes a deformation pattern containing some parameters. We substitute this deformation form to the standard elasticity equation describing spherical elasticity for homogeneous isotropic deformation for compressible structural material. We considered typically, a Blatz-ko material and analysed both the solid and hollow spherical form of this material when the force that cause deformation is internal pressure such that the external environment is stress free. Consequently we determine the stress components as we allow the material to deform. By using Cauchy elasticity we noted that the only non-trivial component of stress is in the radial direction. Substitution in the non-zero component of continuity equation resulted into a non-linear second order partial differential equation for explicit determination of stresses and displacement the model gave rise to a boundary value problem where both the equation and boundary conditions were non-linear. A transformation was introduced which linearized the boundary conditions, this allowed the method of asymptotes. The minimization of the error in sobolove norm helped us to control both the function and its gradient. Consequently, exact solutions of the stresses and displacements at every section of the compressible spherical solid and hollow sphere deforming under internal pressure were determined.

Keywords: Stresses, Blatz-Ko, Rotating Solid, Hollow Spheres

INTRODUCTION

The introduction, history and application of rotating spheres, both solid and hollow are significant in various scientific and engineering fields. A Rotating sphere can be defined as a three-dimensional object where all points on its surface are equidistant from its Centre. This symmetry leads to unique properties in dynamics, particularly in how these objects behave under rotation. The moment of inertia, a key factor in rotational dynamics differs between solid and hollow spheres due to their mass distribution. The study of Spheres dates back to ancient civilizations. The Greeks, particularly Euclid, explored geometric properties of spheres extensively. The concept of a sphere as a solid formed by rotating a circle around an axis was formalized in Euclidean geometry. Over centuries, mathematicians and physicists like Archimedes contributed to understanding the properties of spheres, including volume and surface area calculations. In the 17th century, Isaac Newton's works on motion laid the groundwork for classical mechanics, further enhancing the understanding of rotating bodies. The study of Non-linear rotation in spherical solids and hollow spherical solids involves examining their dynamics behaviour under various conditions. Non-linear effects in rotating systems, such as r-modes in spherical shell, reveal that these modes can carry zero angular momentum while possessing positive energy, challenging traditional beliefs about angular momentum in rotating bodies. For hollow spherical solids, the analysis of thermo-elastic deformation shows that rotational significantly impacts stress distribution and temperature gradients within the material. Rotating spheres are crucial in designing flywheels and gyroscopes. Their predictable rational behaviour aids in stabilizing machinery and vehicles. Understanding the dynamics of solid and hollow spheres informs the designs of sports equipment like balls used in soccer or basketball. The differences in rotation affect how these objects travel through air or roll on surfaces. Celestial bodies like planets and stars can be modeled as Rotating spheres. This modeling helps scientists understand gravitational interactions and rotational dynamics in space. Rotating spheres are studied to understanding fluid flow around objects, which is vital in aerodynamics and hydrodynamics applications Yang *et al*., (2020a). Technologies like MRI utilize principles related to rotating spheres for imaging internal structures within the body. In robotics, understanding how spherical objects rotate assists in designing robots that can navigate through environments effectively. Rotating spheres serve as practical examples in physics education to illustrate concepts such as angular momentum and energy conservation.

Research on the non-linear rotation of spherical solids encompasses a wide range of studies that investigate the dynamics, stability and interactions of these systems in various contexts. Huang (2019) investigated the dynamic response of spherical particles subjected to oscillatory flows, analyzing how non-linear interactions influence particle migration patterns within fluid environments. Hurd *et al.* (2017) conducted experimental research on various shear moduli and diameters using high-speed cameras. They found that the sphere's deformation period measured in their experiment was slightly longer than that obtained by their developed numerical model. They attributed this difference to the additional mass during the sphere's water-entry process. Ahsan, *et al.* (2025) examined the flow behavior and the cuttings transport of non- Newtonian drilling fluid in the

geometry of an eccentric annulus, accounting for what impacts drill pipe rotation might have on fluid velocity, and annular eccentricity on axial and tangential distributions of velocity. They developed a two-phase Eulerian–Eulerian model using computational fluid dynamics to simulate drilling fluid flow and cuttings transport. The study used kinetic theory of granular flow to study the dynamics and interactions of cuttings transport. They modeled Non-Newtonian fluid properties using power law and Bingham plastic formulations. Their simulation results showed a marked improvement in efficiency, as much as 45%, in transport by increasing the fluid inlet velocity from 0.54 m/s to 2.76 m/s, reducing the amount of particle accumulation and changing axial and tangential velocity profiles dramatically, particularly at narrow annular gaps. At a 300 rpm rotation, the drill pipe brought on a spiral flow pattern, which penetrated tangential velocities in the narrow gap that had increased transport efficiency to almost 30% more. Shear-thinning behavior characterizes fluid of which the viscosity, at nearly 50% that of the central core low-shear regions, was closer to the wall high-shear regions. Fluid velocity and drill pipe rotation play a crucial role in optimizing cuttings transport. Higher fluid velocities with controlled drill pipe rotation enhance cuttings removal and prevent particle build-up, thereby giving very useful guidance on how to clean the wellbore efficiently in drilling operations.

Zhang *et al*., (2020) explored turbulent flow around rotating spheres using computational fluid dynamics simulations highlighting how turbulence interacts with spherical bodies under different flow conditions. Chen *et al*,. (2022) focused on modeling heat transfer processes around rotating spheres in viscous fluids, emphasizing how temperature gradients influence overall system stability under non-linear conditions. Zhang *et al*., (2019) studied the temperature and velocity distributions around two identical spheres at a determined vertical distance inside the quiescent air. Their results showed that the lower sphere plays a crucial role in free heat transfer and flow around the higher sphere. Singh and Dash (2015) studied the improvement of natural heat transfer using fin on the surface of a hot sphere in an infinite environment. In their work, they numerically compared the two fin models in terms of thermal performance.

In an analytical study, D'Alessio analytically investigated the unsteady natural convection flow for a hot rotating sphere at high Grashof numbers. His study led to the heat transfer coefficient determining the mixed convection heat transfer around a rotating sphere within a cubical chamber. Zhang *et al*., (2025) analyzed stress distribution and drag effects during deformation cycles of hyperelastic spheres entering water, highlighting coupling between deformation and internal stress fields consistent with Blatz-Ko material behaviour. Yang *et al*., (2020a) compared stress variations on rigid versus hyperelastic spheres, showing visible stress wave ripples on elastic spheres during deformation, consistent with Blatz-Ko material response. Yang *et al*., (2021a) observed elongation of deformation period with increasing sphere density due to slower stress wave propagation in hyperelastic spheres, relevant to compressible Blatz-Ko materials. Zhang *et al*., (2025) validated numerical models with experimental data on cavity profiles and deformation parameters during sphere water entry, consistent with Blatz-Ko material assumptions. Yang *et al*., (2020b) analyzed differences in strain and kinetic energies between rigid and hyperelastic spheres under varying shear moduli and velocities, showing deformation magnitude increase with velocity but period remains constant, consistent with Blatz-Ko material behaviour.

MATERIALS AND METHODS

Solid Sphere

This particular problem to be solved is spherical in nature. Hence all the field equations developed earlier should be converted to spherical coordinates.

Let $\Omega_0 = \{(r,\theta,\phi): 0 \le r \le c, 0 \le \theta \le \pi, 0 \le \phi \le 2\pi\}$ denote the cross section of a solid sphere in its undeformed configuration. The deformation resulting from the rotation of the sphere about its own axis is axisymmetric and takes the point (r,θ,ϕ) at the undeformed configuration to the point (R,Θ,Φ) at the deformed configuration such that,

$$(r,\theta,\phi) \rightarrow (R,\Theta,\Phi)$$

Viz
$$\begin{aligned} R &= R(r) \quad 0 \le r \le c \\ \Theta &= \theta \quad 0 \le \theta \le \pi \\ \Phi &= \phi \quad 0 \le \phi \le 2\pi \end{aligned} \tag{1}$$

Here we assume that
$R(r) \in C^2(0,c)$ Is such that R and its derivatives $\dot{R}$, $\ddot{R}$ are non-negative. We also assume that the sphere is large enough that effects are neglected.

Deformation Gradient Tensor $\bar{F}$

We shall determine the deformation gradient, which describes how material line elements change their length and orientation during deformation.

In spherical co-ordinate the deformation gradient tensor, $\bar{F}$ is given by;

$$\bar{F} = \begin{pmatrix} \frac{\partial R}{\partial r} & \frac{\partial R}{\partial \theta} & \frac{\partial R}{\partial \phi} \\ R\frac{\partial \theta}{\partial r} & \frac{R}{r}\frac{\partial \theta}{\partial \theta} & R\frac{\partial \theta}{\partial \phi} \\ \frac{R}{r}\frac{\partial \phi}{\partial r} & \frac{R}{r}\frac{\partial \phi}{\partial \theta} & \frac{R}{r}\frac{\partial \phi}{\partial \phi} \end{pmatrix} \tag{2}$$

Now $\frac{\partial R}{\partial r} = \dot{R}, \frac{\partial \theta}{\partial \theta} = 1, \frac{\partial \phi}{\partial \phi} = 1.$

All other off terms are zero, so that the deformation gradient tensor becomes

$$\bar{F} = \begin{pmatrix} \dot{R} & 0 & 0 \\ 0 & \frac{R}{r} & 0 \\ 0 & 0 & \frac{R}{r} \end{pmatrix} \tag{3}$$

Left Cauchy-Green Deformation Tensor $\bar{B}$

The Left Cauchy-Green Deformation Tensor $\bar{B}$ is given by;

$$\bar{B} = \bar{F}\bar{F}^T = \begin{pmatrix} \dot{R} & 0 & 0 \\ 0 & \frac{R}{r} & 0 \\ 0 & 0 & \frac{R}{r} \end{pmatrix}\begin{pmatrix} \dot{R} & 0 & 0 \\ 0 & \frac{R}{r} & 0 \\ 0 & 0 & \frac{R}{r} \end{pmatrix}$$

$$\bar{B} = \begin{pmatrix} \dot{R}^2 & 0 & 0 \\ 0 & \left(\frac{R}{r}\right)^2 & 0 \\ 0 & 0 & \left(\frac{R}{r}\right)^2 \end{pmatrix} \tag{4}$$

Where $\bar{F}^T$ is the transpose of $\bar{F}$?

We note here that the trace of $\bar{B}$.

$$tr(\bar{B}) = \dot{R}^2 + \left(\frac{R}{r}\right)^2 + \left(\frac{R}{r}\right)^2$$

$$= \dot{R}^2 + 2\left(\frac{R}{r}\right)^2 \tag{5}$$

The Jacobian, J, of $\bar{B}$ is given by from (3.79) as

$$J = (det\ \bar{B})^{1/2} = \left\{ \dot{R}^2 \begin{vmatrix} \left(\frac{R}{r}\right)^2 & 0 \\ 0 & \left(\frac{R}{r}\right)^2 \end{vmatrix} \right\}^{1/2}$$

$$= \left\{ \dot{R}^2 \left(\frac{R}{r}\right)^4 \right\}^{1/2}$$

$$= \dot{R}\left(\frac{R}{r}\right)^2 \tag{6}$$

In this work, we are considering a Blatz-ko material which represents the general foam rubber. It is characterized by the elastic potential

$$W(\lambda_r,\lambda_\theta,\lambda_\phi)=\frac{\mu}{2}\left[\frac{1}{\lambda_r{}^2}+\frac{1}{\lambda_\theta{}^2}+\frac{1}{\lambda_\phi{}^2}+2\lambda_r\,\lambda_\theta\,\lambda_\phi-5\right] \quad (7)$$

Where $\mu>0$ is the Shear modulus at infinitesimal deformation?

$\lambda_r,\lambda_\theta,\lambda_\phi$ Are the principal stresses. It could be seen that $\lambda_r\,\lambda_\theta\,\lambda_\phi=J$

The principal stress field is given by;

$$\tau_{ii}=\frac{\lambda_i}{\lambda_r\lambda_\theta\,\lambda_\phi}.\frac{\partial W}{\partial\lambda_i}\quad i=r,\theta,\phi \quad (8)$$

Since off diagonal terms are zero.

Now noting that

$$\lambda_r=\dot{R}$$
$$\lambda_\theta=\frac{R}{r} \quad (9)$$
$$\lambda_\phi=\frac{R}{R}$$

From (9) we have;

$$\frac{\partial W}{\partial\lambda_r}=\frac{\mu}{2}\left[-2\lambda_r{}^{-3}+2\lambda_\theta\,\lambda_\phi\right]$$
$$=\frac{\mu}{2}\left[-\frac{2}{\dot{R}^3}+2\left(\frac{R}{r}\right)^2\right] \quad (10)$$
$$\frac{\partial W}{\partial\lambda_\theta}=\frac{\mu}{2}\left[-2\lambda_\theta{}^{-3}+2\lambda_r\,\lambda_\phi\right]$$
$$=\frac{\mu}{2}\left[-2\left(\frac{r}{R}\right)^3+2\frac{\dot{R}R}{r}\right] \quad (11)$$
$$\frac{\partial W}{\partial\lambda_\phi}=\frac{\mu}{2}\left[-2\lambda_\phi{}^{-3}+2\lambda_r\,\lambda_\theta\right]$$
$$=\frac{\mu}{2}\left[-2\left(\frac{R}{r}\right)^3+2\dot{R}\left(\frac{R}{r}\right)\right] \quad (12)$$

Using (6), (7) and (8) in (9) we have the stress components as

$$\tau_{11}=\tau_{RR}=\frac{1}{\left(\frac{R}{r}\right)^2}.\frac{\mu}{2}\left[-\frac{2}{\dot{R}^3}+2\left(\frac{R}{r}\right)^2\right]$$
$$=\frac{r^2}{R^2}\left(\frac{\mu}{r}\right)\left[\frac{-2r^2+2R^2\dot{R}^3}{r^2\dot{R}^3}\right]$$
$$=\frac{\mu}{2}\left[\frac{-2r^2+2R^2\dot{R}^3}{\dot{R}^3R^2}\right]$$
$$=\frac{\mu}{2}.2\left[\frac{-r^2+R^2\dot{R}^3}{\dot{R}^3R^2}\right]$$
$$=\mu\left[\frac{R^2\dot{R}^3}{\dot{R}^3R^2}-\frac{r^2}{R^2\dot{R}^3}\right]$$
$$=\mu\left[1-\frac{r^2}{R^2\dot{R}^3}\right] \quad (13)$$

$$\tau_{22}=\tau_{\theta\theta}=\frac{\mu}{2}.\frac{1}{\dot{R}\left(\frac{R}{r}\right)}\left[-2\left(\frac{r}{R}\right)^3+\frac{2R\dot{R}}{r}\right]$$
$$=\frac{r}{R\dot{R}}.\mu\left[\frac{-r^4+R^4\dot{R}}{rR^3}\right]$$
$$=\mu\left[\frac{-r^4+R^4\dot{R}}{R^4\dot{R}}\right]$$
$$=\mu\left[\frac{R^4\dot{R}}{R^4\dot{R}}-\frac{r^4}{R^4\dot{R}}\right]$$
$$=\mu\left[1-\frac{r^4}{R^4\dot{R}}\right] \quad (14)$$

$$\tau_{33}=\tau_{\phi\phi}=\frac{1}{\dot{R}\left(\frac{R}{r}\right)}.\frac{\mu}{2}\left[-2\left(\frac{r}{R}\right)^3+\frac{2R\dot{R}}{r}\right]$$
$$=\frac{r}{R\dot{R}}.\mu\left[\frac{-r^4+R^4\dot{R}}{rR^3}\right]$$
$$=\mu\left[\frac{-r^4+R^4\dot{R}}{R^4\dot{R}}\right]$$
$$=\mu\left[\frac{R^4\dot{R}}{R^4\dot{R}}-\frac{r^4}{R^4\dot{R}}\right]$$
$$=\mu\left[1-\frac{r^4}{R^4\dot{R}}\right] \quad (15)$$

The continuity equation governing rotation in spherical co-ordinate is given by;

$$R^2\frac{\partial\tau_{RR}}{\partial R}+2R\tau_{RR}-2R\tau_{\phi\phi}+R^3\rho\omega^2=0 \quad (16)$$

Where ω is the angular velocity which here is assumed constant.

ρ is the density of the material in deformed configuration.

Let ρ_0 be density in undeformed configuration. The relation between ρ_0 and ρ is

$$\rho J=\rho_0 \quad (17)$$

Where $J=(det\,\bar{B})^{1/2}=\frac{\dot{R}R^2}{r^2}$

Now using the chain rule of differentiation we have;

$$\frac{\partial\tau_{RR}}{\partial r}=\frac{\partial\tau_{RR}}{\partial R}.\frac{\partial R}{\partial r}=\dot{R}\,\frac{\partial\tau_{RR}}{\partial R}$$
$$\Longrightarrow\quad \dot{R}\,\frac{\partial\tau_{RR}}{\partial R}=\frac{\partial\tau_{RR}}{\partial r}$$
$$\Longrightarrow\quad \frac{\partial\tau_{RR}}{\partial R}=\frac{1}{\dot{R}}\,\frac{\partial\tau_{RR}}{\partial r}$$

Now using (16) and substituting the stress components in (18) we have

$$\frac{R^2}{\dot{R}}\frac{\partial\tau_{RR}}{\partial r}+2R\left[1-\frac{r^4}{R^4\dot{R}}\right]-2R\left[1-\frac{r^4}{R^4\dot{R}}\right]+R^3\rho_0(J^{-1})\omega^2=0$$
$$\frac{R^2}{\dot{R}}\frac{\partial\tau_{RR}}{\partial r}+R^3\rho_0(J^{-1})\omega^2=0$$
$$\frac{R^2}{\dot{R}}\frac{\partial\tau_{RR}}{\partial r}+R^3\rho_0\frac{r^2}{R^2\dot{R}}\omega^2=0$$
$$R\frac{\partial\tau_{RR}}{\partial r}+\rho_0r^2\omega^2=0$$

Now $$\frac{\partial\tau_{RR}}{\partial r}=\frac{\partial}{\partial r}\left[\mu\left(1-\frac{r^2}{R^2\dot{R}^3}\right)\right]$$
$$=-\mu\left[\frac{2r(R^2\dot{R}^3)-r^2(2R\dot{R}^4+3R^2\dot{R}^2\ddot{R})}{R^4\dot{R}^6}\right]$$
$$=-\mu\left[\frac{2rR^2\dot{R}^3-2r^2R\dot{R}^4-3r^2R^2\dot{R}^2\ddot{R})}{R^4\dot{R}^6}\right]$$
$$=-\mu\left[\frac{2r}{R^2\dot{R}^3}-\frac{2r^2}{R^3\dot{R}^2}-\frac{3r^2\ddot{R}}{R^2\dot{R}^4}\right]$$
$$=\mu\left[\frac{3r^2\ddot{R}}{R^2\dot{R}^4}-\frac{2r}{R^2\dot{R}^3}+\frac{2r^2}{R^3\dot{R}^2}\right]$$

Put (18) in (19) to get

$$R\mu\left[\frac{3r^2\ddot{R}}{R^2\dot{R}^4}-\frac{2r}{R^2\dot{R}^3}+\frac{2r^2}{R^3\dot{R}^2}\right]+\rho_0r^2\omega^2=0$$
$$\frac{3r^2\ddot{R}}{R\dot{R}^4}-\frac{2r}{R\dot{R}^3}+\frac{2r^2}{R^2\dot{R}^2}+\frac{\rho_0}{\mu}\omega^2r^2=0$$
$$r\left(\frac{3r\ddot{R}}{R\dot{R}^4}-\frac{2}{R\dot{R}^3}+\frac{2r}{R^2\dot{R}^2}+\frac{\rho_0}{\mu}\omega^2r\right)=0$$
$$\frac{3r^2\ddot{R}}{R\dot{R}^4}-\frac{2}{R\dot{R}^3}+\frac{2r}{R^2\dot{R}^2}+\frac{\rho_0}{\mu}\omega^2r=0$$

Multiply through by $R^2\dot{R}^4$ to get

$$3rR\ddot{R}-2R\dot{R}+2r\dot{R}^2+\propto rR^2\dot{R}^4=0 \quad (18)$$

Where $\propto=\frac{\rho_0\,\omega^2}{\mu}$

Solution of equation (20) gives the displacement R from which the stresses at any point on the Rotating sphere can be determined.

Hollow Cylinder

The method of derivation of the equation for the rotating hollow sphere is the same as above for the solid sphere except that here the boundaries are;

$$R=R(r)\quad a\le r\le c$$
$$\Theta=\theta\quad 0\le\theta\le\pi \quad (19)$$
$$\Phi=\phi\quad 0\le\phi\le 2\pi$$

Here we assume that

$R(r)\in C^2(0,c)$ is such that R and its derivatives $\dot{R}$, $\ddot{R}$ are non-negative. We also assume that the sphere is large enough that effects are neglected.

Deformation Gradient Tensor $\bar{F}$

We shall determine the deformation gradient, which describes how material line elements change their length and orientation during deformation.

In spherical co-ordinate the deformation gradient tensor, $\bar{F}$ is given by;

$$\bar{F}=\begin{pmatrix}\frac{\partial R}{\partial r} & \frac{\partial R}{\partial\theta} & \frac{\partial R}{\partial\phi}\\ R\frac{\partial\theta}{\partial r} & \frac{R}{r}\frac{\partial\theta}{\partial\theta} & R\frac{\partial\theta}{\partial\phi}\\ \frac{R}{r}\frac{\partial\phi}{\partial r} & \frac{R}{r}\frac{\partial\phi}{\partial\theta} & \frac{R}{r}\frac{\partial\phi}{\partial\phi}\end{pmatrix} \quad (20)$$

Now $$\frac{\partial R}{\partial r}=\dot{R},\frac{\partial\theta}{\partial\theta}=1,\frac{\partial\phi}{\partial\phi}=1.$$

All other off terms are zero, so that the deformation gradient tensor becomes

$$\bar{F} = \begin{pmatrix} \dot{R} & 0 & 0 \\ 0 & \frac{R}{r} & 0 \\ 0 & 0 & \frac{R}{r} \end{pmatrix} \quad (21)$$

RESULTS AND DISCUSSION

Rotation of a Solid Sphere

Consider the solid sphere $0 \le r \le c, 0 \le \theta \le \pi, 0 \le \phi \le 2\pi$ rotating freely about its axis with a constant angular velocity, ω.

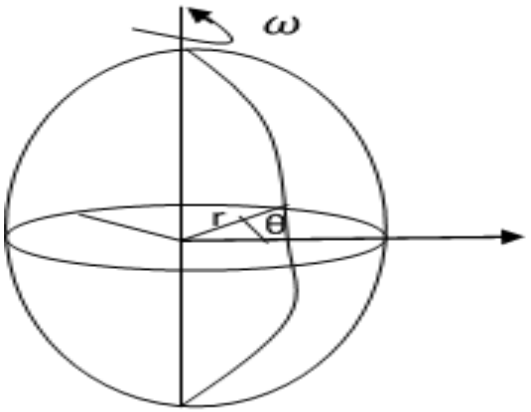

Figure 1: A Spherical Blatz-ko Material Rotating about its Axis with a Constant Angular Velocity, ω

The corresponding boundary conditions are;
at r = 0, $\tau_{RR} = 0 \implies \dot{R}^3(0)R^2(0) = 0$
at r = c, $\tau_{RR} = 0 \implies \dot{R}^3(c)R^2(c) = c^2$
Consequently we need to solve the boundary value problem.

$$\begin{aligned} &3rR\ddot{R} - 2R\dot{R} + 2r\dot{R}^2 + \alpha r R^2 \dot{R}^4 = 0 \\ &\dot{R}^3(0)R^2(0) = 0 \\ &\dot{R}^3(c)R^2(c^2) = 0 \end{aligned} \quad (22)$$

Here both the equation and the boundary conditions are non-linear.
Now let $R^5(r) = g^3(r)$ (23)
Be the solution of the equation satisfying the boundary condition as in (4.1)
Where $g(r)$ belongs to the Sobolev space of order 2.
From (25)

$$5R^4\dot{R} = 3g^2\dot{g}, R = g^{3/5} \quad (24)$$

$$\Rightarrow \dot{R} = \frac{3}{5}g^{-2/5}\dot{g} \quad (25)$$

$$\Rightarrow \ddot{R} = \left(\frac{3}{5}\right)\left[-\frac{2}{5}g^{-7/5}\dot{g}^2\right] + \left[\frac{3}{5}g^{-2/5}\dot{g}\right] \quad (26)$$

$$= \left(\frac{3}{5}\right)\left(-\frac{2}{5}\right)g^{-7/5}\dot{g}^2 + \frac{3}{5}g^{-2/5}\ddot{g} \quad (27)$$

Substituting (26), (27) and (28) in B.V.P (24), we obtain

$$3rg^{3/5}\left[\left(\tfrac{3}{5}\right)\left(\tfrac{-2}{5}\right)g^{-7/5}\dot{g}^2 + \left(\tfrac{3}{5}\right)g^{-2/5}\ddot{g}\right] - 2g^{3/5}\left(\tfrac{3}{5}g^{-2/5}\dot{g}\right) + 2r\left(\tfrac{3}{5}\right)^2\left(g^{-2/5}\right)^2\dot{g}^2 + \propto r(g^{3/5})^2\left[\left(\tfrac{3}{5}\right)g^{-2/5}\dot{g}\right]^4 = 0 \quad (28)$$

$$3r\left(\tfrac{3}{5}\right)\left(\tfrac{-2}{5}\right)g^{-4/5}\dot{g}^2 + 3r\left(\tfrac{3}{5}\right)g^{1/5}\ddot{g} - 2\left(\tfrac{3}{5}\right)g^{1/5}\dot{g} + 2r\left(\tfrac{3}{5}\right)^2 g^{-4/5}\dot{g}^2 + \propto r\left(\tfrac{3}{5}\right)^4 g^{-2/5}\dot{g}^4 = 0 - 3\left(\tfrac{6}{25}\right)rg^4\dot{g}^2 + 3\left(\tfrac{3}{5}\right)rg\ddot{g} - 2\left(\tfrac{3}{5}\right)g\dot{g} - 2r\left(\tfrac{3}{5}\right)^2 g^4\dot{g}^2 + \propto r\left(\tfrac{3}{5}\right)^4 g^2\dot{g}^4 = 0 \quad (29)$$

i.e.

$$3\left(\tfrac{3}{5}\right)rg\ddot{g} - 3\left(\tfrac{6}{25}\right)rg^4\dot{g}^2 - 2\left(\tfrac{3}{5}\right)g\dot{g} - 2r\left(\tfrac{3}{5}\right)^2 g^4\dot{g}^2 + \propto r\left(\tfrac{3}{5}\right)^4 g^2\dot{g}^4 = 0 \quad (30)$$

i.e.

$$3\left(\tfrac{3}{5}\right)rg\ddot{g} - 3\left(\tfrac{6}{25}\right)rg^3\dot{g}^2 - 2\left(\tfrac{3}{5}\right)\dot{g} - 2r\left(\tfrac{3}{5}\right)^2 g^3\dot{g}^2 + \propto r\left(\tfrac{3}{5}\right)^4 g\dot{g}^4 = 0 \quad (31)$$

Consequently the boundary value problem (4.1) reduces to solving;

$$3rg\ddot{g} - 3\left(\tfrac{2}{5}\right)rg^3\dot{g}^2 - 2\dot{g} - 2r\left(\tfrac{3}{5}\right)g^3\dot{g}^2 + \propto r\left(\tfrac{3}{5}\right)^3 g\dot{g}^4 \quad (32)$$

$$g(0) = 0$$

$$\dot{g}(c) = \frac{5}{3}c^{2/3} \quad (33)$$

We note that the transformation made the boundary conditions linear, though the equation is still non-linear.
The direct analytic solution of (30) is not readily feasible. Hence we seek the solution of (30) in $W^{1,2}(0,c)$ the Sobolev space of order two. The space $W^{1,\rho}(0,c)_\rho$ is characterized by absolutely continuous functions.
Now let

$$g(r) = r^{5/3}\left[a_0 + a_1 r^2\right] \quad 0 \le r \le c \quad (34)$$

Be a solution of equation (4.7) where a_0 and a_1 are to be determined such that the boundary conditions are satisfied.
From (31)

$$\dot{g}(r) = \frac{5}{3}r^{2/3}\,a_0 + \frac{11}{3}\,a_1\,r^{8/3} \quad (35)$$

The second boundary condition gives

$$\dot{g}(c) = \frac{5}{3}c^{2/3}\,a_0 + \frac{11}{3}\,a_1\,c^{8/3} = \frac{5}{3}c^{2/3} \quad (36)$$

Which gives a_0 in terms of a_1 as

$$a_0 = \frac{\frac{5}{3}c^{2/3} - \frac{11}{3}a_1\,c^{8/3}}{\frac{5}{3}c^{2/3}} \quad (37)$$

$$= 1 - \frac{11}{5}c^2 a_1 \quad (38)$$

Now, we substitute (32) in (31) and minimize the error.

$$\begin{aligned} g(r) &= r^{5/3}\left[a_0 + a_1 r^2\right] = a_0 r^{5/3} + a_1 r^{11/3} \\ \dot{g}(r) &= \tfrac{5}{3}a_0 r^{5/3} + \tfrac{11}{3}\,a_1\,r^{8/3} \\ \ddot{g}(r) &= \left(\tfrac{5}{3}\right)^2 a_0 r^{2/3} + \left(\tfrac{11}{3}\right)\left(\tfrac{8}{3}\right)\,a_1\,r^{5/3} \end{aligned} \quad (39)$$

Substituting (33) in (30) we obtain the error, where a_0 is replaced as from (32)

$$\varepsilon(r, a_1) = 2r^{\frac{20}{3}} + \propto r^{\frac{74}{3}} + \left(-16r^{\frac{20}{3}} + \frac{104}{3} \propto r^{\frac{80}{3}}\right)a_1 \quad (40)$$

$$+ \left(36r^{\frac{20}{3}} - 6724 \propto r^{\frac{80}{3}}\right){a_1}^2 + 0({a_1}^3) \quad (41)$$

The error is minimum when

$$\frac{\partial}{\partial a_1}//\varepsilon(r_1, a_1)/_{-_{1,2}} = 0 \quad (42)$$

Where $\varepsilon(r, a_1)$ is as in (34);
Substituting (34) into (35) we obtain after computation

$$a_1 = \frac{-91\propto}{200c^2} \quad (43)$$

to the first order in $\propto$.
Consequently we have the solution as

$$g(r) = \tfrac{5}{3}r^{2/3}\left[1 - \tfrac{11}{5}c^2\left(\tfrac{-91\propto}{200c^2}\right)\right] - \tfrac{-91\propto r^{11/3}}{200c^2} \quad (44)$$

$$= \frac{5}{3}\left[1 + \left(\frac{11}{5}\right)\left(\frac{91}{200}\right)\right]r^{2/3} - \frac{91\propto}{200c^2}r^{11/3} \quad (45)$$

But $R = g^{5/3}$

$$= \left\{\frac{5}{3}\left[1 + \frac{11}{5}\left(\frac{91}{200}\right)\right]r^{2/3} - \frac{91\propto}{200c^2}\,r^{11/2}\right\}^{\frac{5}{3}} \quad (46)$$

Rotation of a Hollow Sphere

For the Rotating hollow sphere,
Let $\Omega_0 = \{(r, \theta, \phi): c \le r \le h, 0 \le \theta \le \pi, 0 \le \phi \le 2\pi\}$ denote the cross section of a hollow sphere in its

undeformed configuration. The deformation resulting from the rotation of the sphere about its axis is symmetric and is given by;

$$\begin{aligned} R &= R(r) & c \le r \le h \\ \theta &= \Theta & 0 \le \theta \le \pi \\ \phi &= \Phi & 0 \le \phi \le 2\pi \end{aligned} \quad (47)$$

$(r, \theta, \phi) \rightarrow (R, \Theta, \Phi)$

Such that

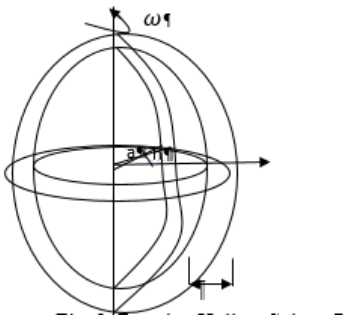

Figure 2: Rotating Hollow Sphere

Following analysis as the case of solid sphere, the resulting boundary value problem is

$$\begin{aligned} 3rR\ddot{R} - 2R\dot{R} + 2r\dot{R}^2 + \alpha r R^2 \dot{R}^4 = 0 \\ \dot{R}^3(c)R^2(c) = c^2 \\ \dot{R}(h)R^2(h) = h^2 \end{aligned} \quad (48)$$

Again we observe that both equation and the boundary conditions are both non-linear.

Now let

$$R^5(r) = g^3(r) \quad (49)$$

So that

$$R(r) = g^{3/5}(r) \quad (50)$$

$$\dot{R}(r) = \frac{3}{5} g^{-2/5}(r)\dot{g}(r) \quad (51)$$

$$\ddot{R}(r) = \frac{3}{5} g^{-2/5}(r)\ddot{g}(r) - \frac{3}{5}\left(\frac{2}{5}\right) g^{-7/5}(r)\dot{g}^2(r) \quad (52)$$

Substituting (4.2.4) – (4.2.6) into (4.2.2) we obtain

$$3\left(\frac{3}{2}\right) r\dot{g}^5\ddot{g} - 3\left(\frac{6}{25}\right) r g^{10}\dot{g}^2 - 2\left(\frac{3}{2}\right) g^{15}\dot{g} + 2\left(\frac{3}{5}\right)^4 r^3\dot{g}^4 \quad (53)$$

$$+ \left(\frac{3}{5}\right)^4 \propto r g^{12}\dot{g}^4 = 0 \quad (54)$$

With boundary conditions reducing to

$$g(c) = \frac{5}{3} c^{2/3} \quad (55)$$

$$g(h) = \frac{5}{3} h^{2/3} \quad (56)$$

Once again we seek the solution of the B.V.P (44) – (46) in the Sobolev space, $W^{1,2}(c, h)$.

Now let

$$g_0(r) = r^{5/3}\left[\frac{a_{-2}}{r^2} + a_0 + a_2 r^2\right] \quad (57)$$

Be such a solution where $a_0,\ a_2, a_{-2}$ are constants such that the boundary conditions must be satisfied.

Since (50) must satisfy the boundary conditions, we have that,

$$a_0 = 1 - \frac{11}{5} a_2(c^2 + h^2) \quad (58)$$

$$a_{-2} = -11 a_2 c^2 h^2 \quad (59)$$

Hence we obtain

$$g_0(r) = r^{\frac{5}{3}} + m(r)a_2 \quad (60)$$

Where

$$m(r) = r^{5/3}\left[r^2 - \frac{11}{5}(c^2 + h^2) - \frac{11c^2h^2}{r^2}\right] \quad (61)$$

Substituting (53) and (54) in the B.V.P we obtain the error $\varepsilon(r, a_2)$ as

$$\varepsilon(r, a_2) = 2r^{20/3} - 2r^{20} + ar^{\frac{24}{3}} + \left\{3\left(\frac{3}{5}\right)\dot{m}r^{27} + 30mr^{23} - 20mr^{\frac{55}{3}} + 30r^{25} - \frac{3}{5}\dot{m}r^{26} + 8\left(\frac{3}{5}\right)\dot{m}r^6 + \left[4\left(\frac{3}{5}\right)\dot{m}r^{24} + 12r^{23}a\right]a_2 + 27\dot{m}\dot{m}r^{\frac{76}{2}} - 54\left(\frac{3}{5}\right)m^2r^{\frac{50}{3}} - 2\left(\frac{3}{5}\right)\dot{m}^2r^{\frac{56}{3}} + 12\left(\frac{3}{5}\right)^2\dot{m}^2r^{\frac{16}{3}} - 24m\dot{m}r^{\frac{53}{3}} - 18m\dot{m}r^{\frac{73}{3}} + \left[6\left(\frac{3}{5}\right)^2 m^2r^{\frac{20}{3}} - 66\dot{m}r^{\frac{64}{3}} + 48\left(\frac{3}{5}\right)m\dot{m}r^{\frac{73}{3}}\right] \propto\right\}a_2^2 + 0(a_2^3) \quad (62)$$

The error is minimum when

$$\frac{\partial}{\partial a_1} //\varepsilon(r_1, a_1)//_{1,2} = 0 \quad (63)$$

Substituting (55) into 56) we obtain

$$a_2 = \frac{-91\propto}{200(c^2 + h^2)} \quad (64)$$

To the first order approximation in $\propto$. Substituting (57) in 53) we obtain

$$g_0(r) \cong r^{5/3}\left\{1 + \frac{91\propto}{200(c^2+h^2)}\left[\frac{11}{5}(c^2+h^2) + \frac{11c^2h^2}{r^2} - r^2\right]\right\} \quad (65)$$

Consequently, we have the deformed radius R as

$$R = r\left\{1 + \frac{91\propto}{200(c^2+h^2)}\left[\frac{11}{5}(c^2+h^2) + \frac{11c^2h^2}{r^2} - r\right]\right\}^{3/5} \quad (66)$$

The corresponding stress components using (67) – (68)

$$\tau_{RR}(r) = \mu\left\{1 - \left[1 + \frac{1001\propto}{200(c^2+h^2)}\left(\frac{1}{5}(c^2+h^2) - \frac{5c^2h^2}{r^2} - 5r^2\right)\right]^{-2}\right\} \quad (67)$$

$$\tau_{\theta\theta}(r) = \tau_{\phi\phi}(r) = \mu\left\{1 - \left[1 + \frac{91\propto}{200(c^2+h^2)}\left(\frac{11}{5}(c^2+h^2) + \frac{11c^2h^2}{r^2} - r^{-2}\right)\right]^{-2}\right\} \quad (68)$$

Discussion

We have analyzed the Blatz-ko spherical solid rotating about its own axis at a constant angular velocity. It is discovered that the model continuity equation resulting from both the solid and hollow cases are the same. Variation came only on the boundary conditions. We have exploited the characteristics of the Sobolev space in the minimization of the errors that occurred. The characteristics here make it possible to control both the function and its derivatives.

CONCLUSION

This research provided an analytical solution for stresses and displacements induced in a typical spherical material. This paper considered both solid and hollow sphere for generalization and use an indirect method, which assumes a deformation pattern containing some parameters. Deformation form was substituted to the standard elasticity equation describing spherical elasticity for homogeneous isotropic deformation for compressible structural material. A Blatz-ko material was typically considered whose elastic potentials is stated in equation (3.28). This research analyzed both the solid and hollow spherical form of this material when the force that cause deformation is internal pressure such that the external environment is stress free. Consequently we determine the stress components as we allow the material to deform. By using Cauchy elasticity we noted that the only non-trivial component of stress is in the radial direction. Substitution in the non-zero component of continuity equation resulted into a non-linear second order partial differential equation for explicit determination of stresses and displacement the model gave rise to a boundary value problem where both the equation and boundary conditions were non-linear. We introduced a transformation which linearized the boundary conditions, this allowed the method of asymptotes. The minimization of the error in sobolove norm helped us to control both the function and its gradient. Consequently, exact solutions of the stresses and displacements at every section of the compressible spherical

solid and hollow sphere deforming under internal pressure were determined.

REFERENCES

Ahsan, M.; Fahad, S.; Butt, M.S. (2025) Computational Fluid Dynamics Simulation and Analysis of Non-Newtonian Drilling Fluid Flow and Cuttings Transport in an Eccentric Annulus. Mathematics, 13, 101.

Chen, Z., Yang, L. M., Shu, C., Zhao, X., Liu, N. Y., and Liu, Y. Y., 2021, "Mixed Convection between Rotating Sphere and Concentric Cubical Enclosure," Phys. Fluids, 33(1), p. 013605.

D'Alessio, S. J. D., (2018), "An Analytical Study of the Early Stages of Unsteady Free Convective Flow From a Differentially Heated Rotating Sphere at Large Grashof Numbers," Int. J. Comput. Methods Exp. Meas., 7(1), pp. 57–67.

Huang, Y., Xia, Z., Wan, M., Shi, Y. & Chen, S. 2019 Hyste resis behavior in spanwise rotating plane Couette flow with varying rotation rates. Phys. Rev. Fluids 4 (5), 052401.

Hurd, R. C., Belden, J. L., Jandron, M. A., Tate Fanning, D., Bower, A. F., & Truscott, T. T. (2017). Water entry of deformable spheres. *Journal of Fluid Mechanics*, *824*, 912–930.

Singh, B., and Dash, S. K., (2015), "Natural Convection Heat Transfer From a Finned Sphere," Int. J. Heat Mass Transfer, 81, pp. 305–324.

Yang, L., Wei, Y., Wang, C., Xia, W., & Li, J. (2020a). Numerical investigations on the deformation styles and stress distributions of hyperelastic/viscoelastic spheres during water entry. Journal of Applied Physics, 127(6), 064901.

Yang, L., Wei, Y., Wang, C., Xia, W., Li, J., & Chen, C. (2020b). Numerical study on the deformation behaviors of elastic spheres during water entry. *Journal of Fluids and Structures*, *99*, 103167.

Zhang, S., Xia, Z., Zhou, Q. & Chen, S. 2020 Controlling flow reversal in two-dimensional Rayleigh–Bénard convection. J. Fluid Mech. 891, R4.

Zhang, L., Xie R., and Jia, H. (2025). Numerical Research of the Water Entry of Hyper elastic Spheres within Low Froude Numbers. *Journal of Applied Fluid Mechanics*, Vol. 18, No. 3, pp. 821-834

Zhang, J., Zhen, Q., Liu, J., and Lu, W.-Q., 2019, "Effect of Spacing on Laminar Natural Convection Flow and Heat Transfer from Two Spheres in Vertical Arrangement," Int. J. Heat Mass Transfer, 134, pp. 852–865.